Molecular Crystals and Liquid Crystals
Publication details, including instructions for authors and subscription information:
http://www.tandfonline.com/loi/gmcl16

Electric Field-Induced Deformations in Oriented Liquid Crystals of the Nematic Type

Hans Gruler [a] & Gerhard Meier [a]

[a] Institut für Angewandte Festkörperphysik der Fraunhofer-Gesellschaft, Freiburg i. Br., Germany

Version of record first published: 21 Mar 2007.

To cite this article: Hans Gruler & Gerhard Meier (1972): Electric Field-Induced Deformations in Oriented Liquid Crystals of the Nematic Type, Molecular Crystals and Liquid Crystals, 16:4, 299-310

To link to this article: http://dx.doi.org/10.1080/15421407208082793

Molecular Crystals and Liquid Crystals. 1972. Vol. 16, pp. 299–310

Electric Field-Induced Deformations in Oriented Liquid Crystals of the Nematic Type

HANS GRULER and GERHARD MEIER

Institut für Angewandte Festkörperphysik der Fraunhofer-Gesellschaft
Freiburg i. Br.
Germany

Received May 27, 1971; *in revised form August* 7, 1971

Abstract—The influence of an electric field on nematic liquid crystals is investigated for several orientations of the liquid crystal. We give a theoretical treatment of the normal deformation that arises from the interaction of the electric field with the dielectric anisotropy. Our experimental deformations show relatively good agreement with the calculated values. Some anomalous deformations were also investigated. Conditions and threshold voltages for Williams domains are discussed. If the undisturbed optical axis is parallel to the applied electric field and the dielectric anisotropy is positive, no Williams domains appear. This result is in agreement with the Carr–Helfrich model.

1. Introduction

The present work deals with the effect of an electric field on oriented liquid crystals.

The investigations of Gruler and Meier[1] on azo- and azoxy-compounds have shown that Williams domains[2,3] appear for both positive and negative dielectric anisotropy $\Delta\epsilon$. $\Delta\epsilon = \epsilon_1 - \epsilon_2$, where ϵ_1 denotes the principal dielectric constant parallel and ϵ_2 perpendicular to the optical axis. In their experiments the undisturbed optical axis of the liquid crystal, $\mathbf{L}_0$, was perpendicular to the applied electric field. In the present paper we report on further work carried out with nematic liquid crystals, where the undisturbed optical axis was also made parallel to the applied electric field. For this case the electrodes were treated with lecithine to make $\mathbf{L}_0 \| \mathbf{E}$. Different types of deformations are to be distinguished: The so-called "normal deformation" takes place in electrically non-conducting liquid crystals or at high frequencies[4,18] and is governed only by the dielectric anisotropy. Various " anomalous deformations " also occur due to additional orientation processes that arise from the electric conductivity. Among these anomalous deformations we shall discuss the Williams domains and a special d.c. instability.(5)

2. Normal Deformation

2.1. Theory

The normal deformation can be described by a free energy G. The following description is analogous to A. Saupe's work(6) on magnetic field effects.

$$G = \tfrac{1}{2}\int_V \left\{[k_{11}\cos^2(\varphi+\varphi_R)+k_{33}\sin^2(\varphi+\varphi_R)]\left(\frac{\mathrm{d}\varphi}{\mathrm{d}x}\right)^2 - \mathbf{D}\cdot\mathbf{E}\right\}\mathrm{d}\tau \quad (1)$$

k_{11} and k_{33} are the elastic constants. **D** and **E** are the displacement and electric field vectors. φ is the angle between the director vector and $\mathbf{L}_0$ and depends upon the location in the sample. φ_R is the angle between $\mathbf{L}_0$ and the boundary surfaces.

For the electric field case the following additional conditions must be considered.

$$\operatorname{div}\mathbf{D} = 0. \quad (2)$$

This holds when the effect of space charge can be neglected.

$$\operatorname{curl}\mathbf{E} = 0 \quad (3)$$

$$U = \int_{x_0} \mathbf{E}\,\mathrm{d}x. \quad (4)$$

For small dielectric anisotropies the electric field is uniform to a very good approximation. The following Eq. (5) describes the deformation in the sample for a uniform electric field. The solution $\varphi(x)$ is such that G is an extreme value.

$$\int_0^{x\le x_0/2}\mathrm{d}x = \int_0^{\varphi\le\varphi_M}\left\{\frac{k_{11}\cos^2(\varphi+\varphi_R)+k_{33}\sin^2(\varphi+\varphi_R)}{\epsilon_0(\epsilon_1-\epsilon_2)E^2(\sin^2(\varphi_M+\varphi_R)-\sin^2(\varphi+\varphi_R))}\right\}^{1/2}\mathrm{d}\varphi \quad (5)$$

In the development of Eq. (5) we imposed a boundary condition requiring φ to have the maximum value φ_M in the center. We now have a relationship between the electric field strength and the deformation $\varphi(x)$.

TABLE 1

$\epsilon_1 - \epsilon_2$	$U_{0\epsilon}$	ν	n_1	κ	Transformation
>0	$\pi\left(\frac{k_{11}}{\epsilon_0(\epsilon_1-\epsilon_2)}\right)^{1/2}$	$\frac{n_e^2-n_o^2}{n_o^2}$	n_o	$\frac{k_{33}-k_{11}}{k_{11}}$	$\Phi = \varphi + \varphi_R$
<0	$\pi\left(\frac{k_{33}}{\epsilon_0(\epsilon_2-\epsilon_1)}\right)^{1/2}$	$\frac{n_o^2-n_e^2}{n_e^2}$	n_e	$\frac{k_{11}-k_{33}}{k_{33}}$	$\Phi = \varphi + \varphi_R \pm \frac{\pi}{2}$

A threshold voltage condition can only exist for $\varphi_R = 0$ and $\varphi_R = \pi/2$.

$$U_{0\epsilon} = E_{0\epsilon} x_0 = \pi\left(\frac{k_{11}}{\epsilon_0(\epsilon_1-\epsilon_2)}\right)^{1/2} \quad \text{for} \quad \varphi_R = 0$$
$$U_{0\epsilon} = E_{0\epsilon} x_0 = \pi\left(\frac{k_{33}}{\epsilon_0(\epsilon_2-\epsilon_1)}\right)^{1/2} \quad \text{for} \quad \varphi_R = \frac{\pi}{2} \tag{6}$$

The simplest way to verify whether a normal deformation is taking place is to measure the optical phase difference d between light polarized in the y-direction and the z-direction.

$$d = \frac{1}{\lambda}\int_{-x_0/2}^{+x_0/2} (n_o - n(x))\,dx$$
$$n(x) = n_e n_o (n_e^2 \sin^2(\varphi + \varphi_R) + n_o^2 \cos^2(\varphi + \varphi_R))^{-1/2}$$

n_o is the ordinary and n_e the extraordinary refractive index.

The zero-field phase difference is subtracted from these measurements to get δ.

$$\delta = d(E) - d(0) = \frac{x_0 n_e n_o}{\lambda n_1}\left\{(1+\sin^2\varphi_R)^{1/2} - \frac{2}{\pi}\frac{E}{E_{0\epsilon}}\cdot\int_{\Phi_R}^{\Phi_M}\frac{(1+\kappa\sin^2\Phi)^{1/2}\,d\Phi}{(1+\nu\sin^2\Phi)^{1/2}(\sin^2\Phi_M - \sin^2\Phi)^{1/2}}\right\} \tag{7}$$

The symbols used in Eq. (7) are defined in Table 1.
The first two terms in a series expansion of $\delta\lambda n_1/x_0 n_e n_o$, valid only when $\varphi_R = 0$, $\pi/2$, are

$$\frac{\delta\lambda n_1}{x_0 n_e n_o} = \nu\frac{E-E_{0\epsilon}}{E_{0\epsilon}}\frac{1}{\kappa+1} - \nu\frac{1}{(\kappa+1)^2}\left(3+\tfrac{9}{4}\nu - \tfrac{5}{4}(\kappa+1)\right)\left(\frac{E-E_{0\epsilon}}{E_{0\epsilon}}\right)^2 + \ldots \tag{8}$$

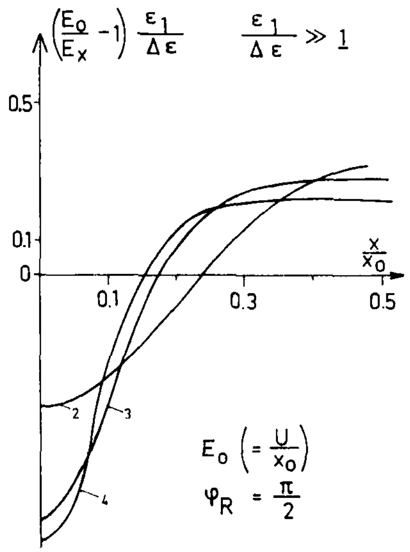

Figure 1. Calculated nonuniform macroscopic electric field E_x in the sample for different deformations $\varphi_0(x;\ U)$.

For larger $\Delta\epsilon$, where the electric field can no longer be considered as uniform, we can still approximately calculate $\varphi(x)$. From Eq.s (2), (3), and (4) we get

$$E(x) = E_0(1 + a(\sin^2\varphi_0 - \eta_2) + \dots)^{-1}$$

$$E_0 = \frac{U}{x_0} \qquad \eta_2 = \frac{2}{x_0}\int_0^{x_0/2} \sin^2\varphi_0 \, dx$$

$$a = \begin{cases} \dfrac{\epsilon_2 - \epsilon_1}{\epsilon_2} & \text{for} \quad \varphi_R = 0 \\ \dfrac{\epsilon_1 - \epsilon_2}{\epsilon_1} & \phantom{\text{for}} \quad \varphi_R = \dfrac{\pi}{2} \end{cases} \tag{9}$$

where $\varphi_0(x)$ is the calculated deformation for the case of a uniform electric field. Figure 1 shows the nonuniform field expected for several values of the assumed electric field. The deformation $\varphi_0(x)$ can be estimated from Fig. 2 for different reduced voltages $U/U_{0\epsilon}$.

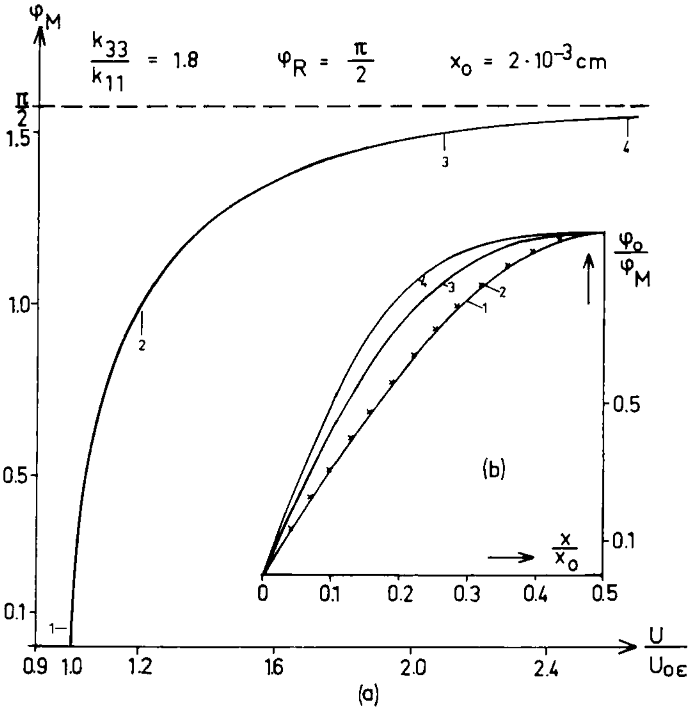

Figure 2. (a) Deformation angle in the center of the sample φ_M *vs* reduced voltage $U/U_{0\epsilon}$; (b) Deformation angle φ_0 *vs* location in the sample. The numbered curves correspond to the different reduced voltages that are indicated in Fig. 2 (a). From Eq. 5 we get $\sin(\pi x/x_0) = \sin\varphi_0/\sin\varphi_M$ for small φ_M.

2.2. Experimental Results

Normal deformation is easily distinguished from anomalous deformation in a wedge-shaped geometry. Between crossed polarizers normal deformations show regular interference bands which are seen as straight lines and shift as a whole when the voltage is increased above threshold. For anomalous deformation the bands are no longer straight.[7]

Figure 3(a) shows the measured δ as function of voltage for a nematic liquid crystal having a small $\Delta\epsilon$. Ignoring the rounding off at low voltages the threshold voltage is defined by the indicated extrapolation.

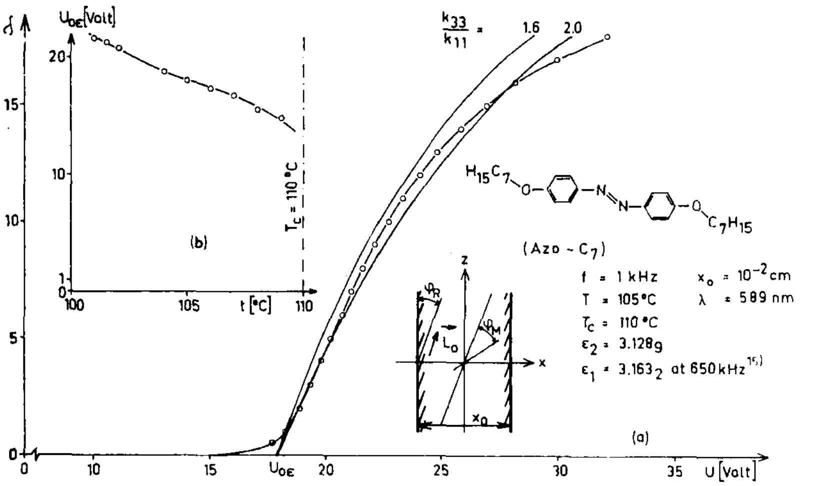

Figure 3. (a) Measured and calculated phase differences δ for different voltages. The experimental curve was taken in the direction of increasing voltage (~1 V/min.). With decreasing voltage the rounding off near the threshold voltage $u_{0\epsilon}$ was more pronounced; (b) Temperature dependence of $U_{0\epsilon}$.

Zwetkoff[4,18] has shown the threshold value to be independent of sample thickness for $\varphi_R = \pi/2$ in mixture of PAA and cinnamic acid.[4] We have also found this to be true for $\varphi_R = 0$ on 50–200 μ thick samples of 4,4′-di-heptoxyazobenzene. We get particularly well oriented samples with $\varphi_R = 0$ by rubbing the surfaces with 4,4′-di-ethoxyazoxybenzene followed by a solvent rinse. Chatelain[19] made a similar observation which is described in his thesis.

Furthermore, we have found the threshold voltage to be independent of frequency up to 3 kHz. A small change in $U_{0\epsilon}$ was observed from 3–30 kHz (see also Ref. 1, Fig. 5). A structural relaxation as predicted by the Orsay Group[20] could explain this change in $U_{0\epsilon}$.

The temperature dependence of $U_{0\epsilon}$ for azo-C_7 is shown in Fig. 3(b). The close agreement of the measured and calculated curves in Fig. 3(a) verify that a normal deformation has taken place. The ratio of elastic constants k_{33}/k_{11} obtained from the calculated curves falls between 1.6 and 2.0. The measured ratio in the case of a magnetic field is 1.5 ± 0.2.[8] The calculated curve is in reasonably good agreement with experiment up to $U = 1.5\ U_{0\epsilon}$.

For most materials, the region of agreement between theory and experiment generally becomes larger with decreasing temperature; azo-C_7, however, is an exception.[8] For magnetic fields the agreement between theory and experiment is always better.[8]

For larger voltages there is a significant departure from theory. The approximations made for small deformations no longer apply.

Saupe[6] believes statistical orientational fluctuations can be responsible for this high field discrepancy. This is also in the right direction to explain the better agreement at lower temperatures. Since agreement is better with magnetic fields, we believe that the electric current produces additional orientational fluctuations. These fluctuations would also explain the smoothing of the predicted discontinuous threshold behaviour.

For larger values of $\Delta\epsilon$, the influence of the resulting nonuniform electric field can be significant. The measured and calculated behaviour of the cyano compound, where $\Delta\epsilon$ is approximately 14,[9] is shown in Fig. 4.

The influence of the nonuniform electric field is easily understood. At an electric field strength slightly above the threshold value, the deformation in the middle of the sample shows a large change for a small change in electric field strength. The electric field will then be smaller in the middle, which will produce a correspondingly smaller

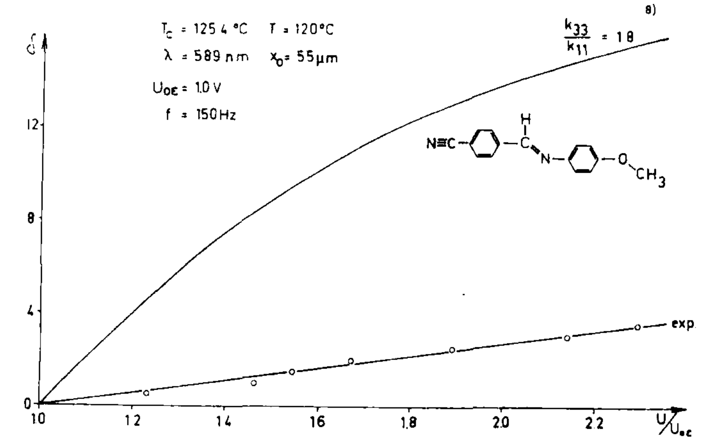

Figure 4. δ *vs* reduced voltage $U/U_{0\epsilon}$ for the indicated cyano compound (large $\Delta\epsilon$). The calculated curve was obtained assuming a uniform electric field.

deformation. We therefore expect for the same reduced voltage $U/U_{0\epsilon}$ deformations to be smaller when $\Delta\epsilon$ is large.

3. Anomalous Deformations

3.1. Williams Domains†

Anomalous deformations can occur in a conducting nematic liquid crystal. The Williams domains are characterized by striped patterns.[2,7] These are easily seen between crossed polarizers with monochromatic light in a polarizing microscope. The threshold voltage $U_{0\sigma}$ is defined as the voltage where the first interference figure appears.[7] This voltage is only very slightly dependent on sample thickness and temperature. Helfrich[10] has calculated the threshold voltage from anisotropic conductivity, dielectric constant, and viscosity data. For PAA, this value agrees very well with the experimental threshold voltage.

We have made further investigations of Williams domains. A summary of our observations is given below.

(i) Williams domains do not appear when $\mathbf{L}_0 \| \mathbf{E}$ and $\Delta\epsilon \geqslant 0$.

(ii) Williams domains appear only up to a cut-off frequency f_c.[5]

(iii) The Williams domains give way to the dynamic scattering mode only when $\Delta\epsilon < 0$.[11] The various orientations at the boundary have no influence on the dynamic scattering mode.

Statement (i) is very important for the understanding of Williams domains and it is based on the following experimental results:

(a) In Fig. 8 ($\Delta\epsilon > 0$, $\mathbf{L}_0 \| \mathbf{E}$) no Williams domains appear.

(b) In Figs. 7(a) and 7(b) ($\Delta\epsilon > 0$, $\mathbf{L}_0 \perp \mathbf{E}$) the Williams domains disappear as the voltage is raised.

(c) In Fig. 6(a) ($\Delta\epsilon < 0$, $\mathbf{L}_0 \| \mathbf{E}$) the threshold voltage can be reached only in one direction. As the voltage is raised from zero, Williams domains appear suddenly when the voltage equals $U_{0\epsilon}$ ($U_{0\sigma} < U_{0\epsilon}$). If the voltage is now lowered, the domains do not disappear until the voltage equals $U_{0\sigma}$ (see arrows in Fig. 6(a)).

† Williams domains are also treated experimentally in Ref. 5 and theoretically in Ref. 21.

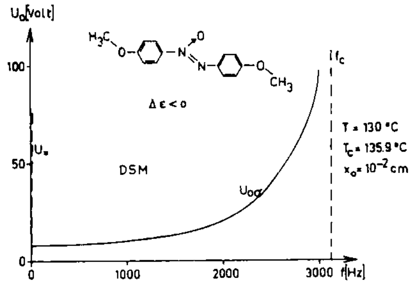

Fig. 5. $\epsilon_1 < \epsilon_2$ and $\mathbf{L}_0 \perp \mathbf{E}$.

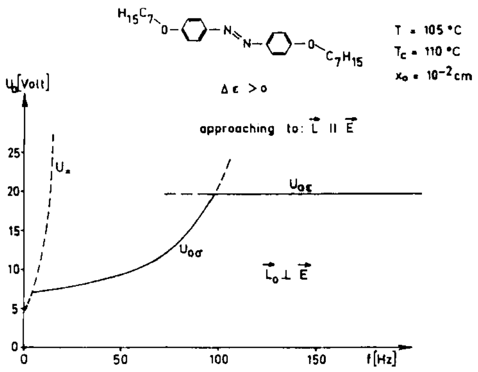

Fig. 7(a). $\epsilon_1 > \epsilon_2$ and $\mathbf{L}_0 \perp \mathbf{E}$.

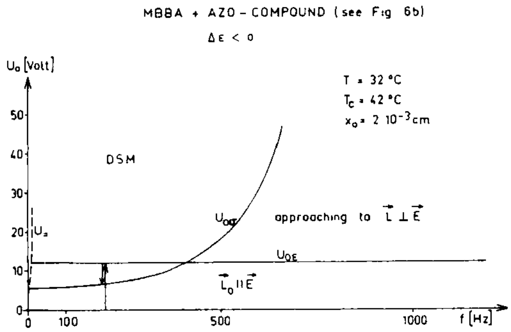

Fig.6(a). $\epsilon_1 < \epsilon_2$ and $\mathbf{L}_0 \| \mathbf{E}$.

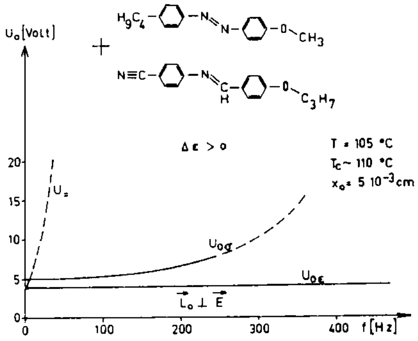

Fig. 7(b). $\epsilon_1 > \epsilon_2$ and $\mathbf{L}_0 \perp \mathbf{E}$.

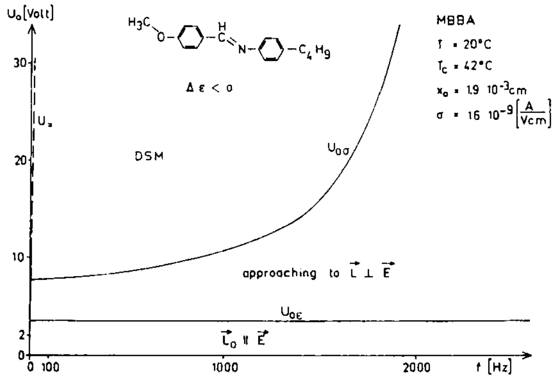

Fig. 6(b). $\epsilon_1 < \epsilon_2$ and $\mathbf{L}_0 \| \mathbf{E}$.

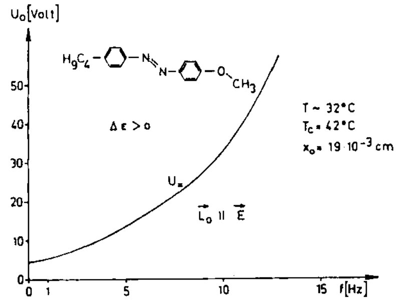

Fig. 8. $\epsilon_1 > \epsilon_2$ and $\mathbf{L}_0 \| \mathbf{E}$.

Figures 5–8. Frequency dependence of threshold voltages.

4. Discussion

According to the Carr[12]–Helfrich model, Williams domains can arise from anisotropy of the electric conductivity. (For all known cases, $\Delta\sigma = \sigma_1 - \sigma_2 > 0$[13] for nematic liquid crystals). In a deformed layer (see Figs. 10(a) and 10(b)) real space charges are created due to the σ-anisotropy.[12] In an electric field such a real space charge produces a fluid flow.

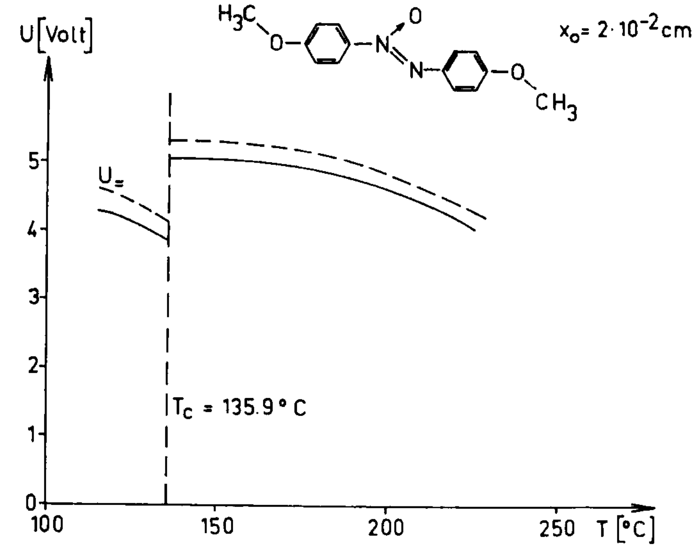

Figure 9. Threshold voltage $U_=$ of the d.c. instability *vs* temperature for *p*-azoxyanisole. Solid line from the kink in the d.c. current-voltage curve and dashed line from observation of dust particle motion in microscope.

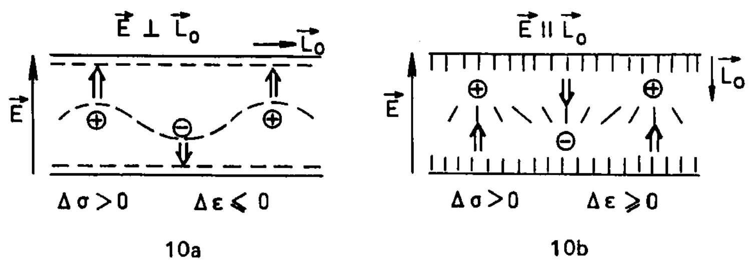

Figure 10. Real space charge and fluid flow produced by small deformations in two different oriented nematic liquid crystal geometrics.

In Fig. 10(a) the system is unstable because the fluid flow reinforces the deformation. This instability gives rise to the Williams domains.

In Fig. 10(b) the system is stable because the shear torque coefficient K_2[14] is negligibly small. (For PAA $K_2 = -0.05$ at 120 °C). Williams domains would be predicted, however, in this geometry for large negative values of K_2. Positive values of K_2 can only contribute to the weakening of the deformation.

4.1. DC Instability

An additional instability that has nothing to do with the nematic phase occurs at d.c. or very low frequencies. It is characterized by the occurrence of very strong fluid flow. This flow can be detected by the motion of added dust or resin particles, by the flow birefringence or by the kink in the measured d.c. current-voltage curve.[1] A typical photograph of this instability has been published by the Orsay Group.[5] We observed this instability for all cases shown in Figs. 5–8 as well as in the isotropic phase (Fig. 9).

4.2. Further Instabilities

Other types of instabilities have been observed, but have not yet been characterized. An example is a grid pattern observed in the azo-compound of Fig. 8 at high voltages and low frequencies (55 V at 30 Hz with $x_0 = 19\,\mu$). The threshold voltage for this grid pattern is not very well reproducible. Nothing is presently known about the mechanism for producing this pattern.

Acknowledgement

We should like to thank Dr. H. Kelker for the azo-compound[16] used in our experiments and Dr. T. Scheffer for helpful discussions.

REFERENCES

1. Gruler, H. and Meier, G., Third Intern. Liq. Cryst. Conf. Berlin 1970 *Mol. Cryst. and Liq. Cryst.* **12**, 289 (1971).
2. Williams, R., *J. Chem. Phys.* **39**, 384 (1963).
3. Fréedericksz, V. and Zolina, V., *Disc. Faraday Soc.* **29**, 919 (1933).
4. Zwetkoff, V., *Acta Physicochimica U.R.S.S.* **6**, 865 (1937) (in German).
5. Orsay Liquid Crystal Group Third Intern. Liq. Cryst. Conf. Berlin 1970 *Mol. Cryst. and Liq. Cryst.* **12**, 251 (1971).

6. Saupe, A., *Z. Naturforschg.* **15a,** 815 (1960).
7. Kassubek, P., Diplomarbeit, Freiburg University 1966.
8. Gruler, H., in preparation.
9. Heilmeier, G. H., Zanoni, L. A. and Goldmacher, J. E., in " Liquid Crystals and Ordered Fluids " (Amer. Chem. Soc. Publication 1970) p. 215.
10. Helfrich, W., *J. Chem. Phys.* **51,** 4092 (1969).
11. Heilmeier, G. H., Zanoni, L. A. and Barton, L. A., *Proc. IEEE* **56,** 1162 (1968).
12. Carr, E. F., *Mol. Cryst. and Liq. Cryst.* **7,** 253 (1969).
13. Svedberg, T., *Ann. Physik* **44,** 1121 (1914); *Ann. Physik* **49,** 437 (1916).
14. Helfrich, W., *J. Chem. Phys.* **50,** 100 (1969).
15. Maier, W. und Meier, G., *Z. f. Phys. Chemie,* **13,** 251 (1957); *Z. f. Elektrochemie* **65,** 556 (1961).
    Meier, G., Thesis, Freiburg, University 1960.
16. Kelker, A., Scheuerle, B., Hatz, R. und Bartsch, W., *Angew. Chem.* **82,** 984 (1969); *Angew. Chem. Internat. Edit.* **9,** 962 (1970).
17. Fréedericksz, V. und Zwetkoff, V., *Acta Physicochimica U.R.S.S.* **3,** 879 (1935) (in German).
18. Fréedericksz, V. und Zwetkoff, V., *Acta Physicochimica U.R.S.S.* **3,** 895 (1935) (in German).
19. Chatelain, M. P., Thesis, Paris University 1937.
20. Orsay Liquid Crystal Group, *J. Chem. Phys.* **51,** 816 (1969).
21. Dubois-Violette, E., de Gennes, P. G. and Parodi, O., *J. Physique* **32,** 305 (1971).